

Experimental Study of Realizing a Low-Noise Injection-Locked Magnetron Based on a Switch-Mode Power Supply

Shaoyue Wang¹, Xiaojie Chen², Yan Zhao¹, Zhongqi He¹, Haoming He¹, Hai Huang¹, Liping Yan¹ and Changjun Liu¹

¹*School of Electronics and Information Engineering, Sichuan University, Chengdu, China*

²*The High People's Court of Guangxi Autonomous Region, Nanning, China*
cjliu@ieee.org

Abstract—Injection-locked magnetrons (ILMGT) are potential candidates in various industrial applications, for example, wireless power transmission. Generally, the output phase and amplitude stability of an ILMGT are influenced by the voltage or current ripple of its power supply. Thus, a high-performance ILMGT cannot exist without an excellent power supply. Switch-mode power supply (SMPS) has the advantages of being compact, high-efficiency, and high-controllability, but it also has a high-ripple and noisy output. Our study is to depress anode voltage ripple without excessive volume and complexity increase. A novel ripple reduction method is proposed. The peak-to-peak value of the SMPS's voltage ripple is reduced from 282 V to 29 V. The output phase jitter of the ILMGT is suppressed from 49° to 0.7° when the injection ratio is 0.13. Besides, the 100-Hz noise is almost completely eliminated without any 100-Hz LC filter. This study provides a reference to establish a compact and low-noise ILMGT system based on commercial SMPSs.

Keywords—Anode voltage ripple, compact, injection-locked, S-band, switch mode power supply, magnetron

I. INTRODUCTION

Microwave applications, such as microwave wireless power transmission (MWPT), microwave phase-controlled arrays, partial accelerators, and so on, have attracted more and more attention nowadays [1]-[4]. Magnetrons are potential microwave sources with the advantages of high efficiency, low cost, and compact size [5]. Besides, injection-locked magnetrons (ILMGT) overcome the free-running magnetrons' defect of random output phase and noisy output spectrum and have attracted great interest [6]. However, the output phase and amplitude stability of an ILMGT are also influenced by its power supply [7]. Researchers have conducted extensive studies to improve the ILMGT's output characteristic.

One aspect is to improve the power supply to reduce magnetrons' output noise. Mitani *et al.* found cutting off the filament current of a magnetron will reduce the magnetron's output noise and realize a narrowband spectrum [8]. Liu. *et al.* carried out an injection-locked magnetron system with ultra-high injection gain and high-stability output characteristics based on a homemade analog power supply [9]. Chen *et al.* theoretically analyzed and experimented and found that suppressing the voltage ripple of the power supply will significantly enhance the output purity of a magnetron [10]. Tsong-Shing Lee combined the filament-heating and cavity-driven circuit of a power supply with gain-frequency regulation control and achieved nearly constant power operation [11]. Another aspect is to apply a closed-loop control. Seong Tae Han *et al.* reduced the phase jitter of a magnetron by applying a low ripple high voltage power supply and a phase-locked circuit [12]. Chen *et al.* realized a solid-source-like performance dual-way power combining

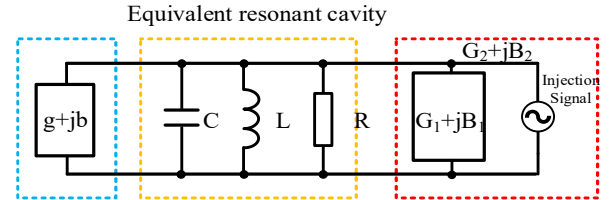


Fig. 1. Equivalent circuits of a magnetron's resonant cavity.

system based on magnetrons with an injection-locking technique and phase-locked loop (PLL), achieving phase jitter as low as $\pm 0.5^\circ$ [13]. However, existing methods also have some defects. An analog power supply always has a bulky size and low efficiency, and a PLL will increase the complexity of the whole system.

In this paper, an experimental study on voltage ripple suppression of a commercial switch-mode power supply (SMPS) is carried out. We proposed a novel voltage suppression module. This module has the advantages of compact size and low complexity. We combined existing methods and our new module to improve a commercial SMPS. The peak-to-peak value of the SMPS's voltage ripple is reduced from 282 V to 29V, and the phase jitter is reduced to 0.8% of the original value. This experimental study provides a new idea for improving the output characteristic of an ILMGT, and it is suitable for various applications that desire to improve the performance of ILMGTs.

II. THEORETICAL ANALYSIS OF ILMGTs

A. ILMGT Under the Influence of Anode Voltage Ripples

According to equivalent circuit theory, a magnetron with an injection signal can be described as a circuit as shown in Fig. 1. The equivalent circuit includes the equivalent electronic admittance is $g+jb$; L , C , and R are the equivalent oscillating circuit parameters; the equivalent load admittance is G_1+jB_1 . The voltage and current of the injection source are V_{inj} and I_{inj} , respectively. The injection signal of an ILMGT can be considered as an equivalent load. We will represent the equivalent load admittance G_2+jB_2 of an ILMGT:

$$G_2 + jB_2 = \frac{I_{RF0} e^{j\omega_c t} - I_{inj} e^{j\omega_{inj} t}}{V_{RF0} e^{j\omega_c t} + V_{inj} e^{j\omega_{inj} t}} = \frac{I_{RF0}}{V_{RF0}} \left(\frac{1 + \frac{I_{inj}}{I_{inj}} e^{j(\omega_{inj} - \omega_c)t}}{1 + \frac{V_{inj}}{V_{RF0}} e^{j(\omega_{inj} - \omega_c)t}} \right) \quad (1)$$

$$\approx G_1 [1 - 2\rho e^{j\theta}] = G_1 - 2G_1 \rho \cos \theta - j2G_1 \sin \theta$$

where $\theta = (\omega_{inj} - \omega_c)t$ is the phase difference between the magnetron's output and injected signal, and the injection ratio ρ is defined as $\rho = \sqrt{P_{inj} / P_{RF0}} = V_{inj} / V_{RF0}$. ω_{inj} and ω_c are the

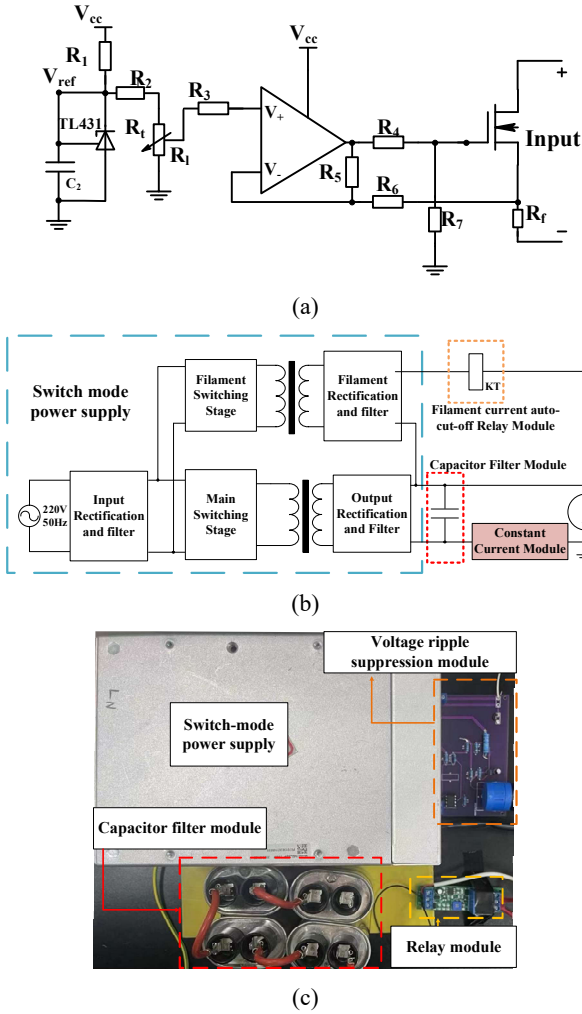


Fig. 2. (a) Diagram of the designed CRE. (b) Structure diagram of the switch-mode power supply. (c) Photograph of the switch-mode power supply.

frequency of the injection signal and the magnetron under free-running state, respectively. Then, the equation of the equivalent circuit shown in Fig. 1 is obtained:

$$g + jb = \frac{1}{R} + j\omega_c C + \frac{1}{j\omega_c L} + 2G - 2G\rho \cos \theta - j2G\rho \sin \theta \quad (2)$$

According to J. C. Slater's work [14], the equivalent electronic admittance of the magnetron is given as follows:

$$g = \frac{1}{R} \left(\frac{V_{dc}}{V_{RF}} - 1 \right) \quad (3)$$

$$b = b_0 + g \tan \alpha \quad (4)$$

Combining (2)-(4), we will have:

$$\frac{d\theta}{dt} = \omega_{inj} - \omega_c - \frac{V_{inj}\omega_0}{V_{RF}Q_{ext}} \sin \theta \quad (5)$$

$$\omega = \omega_0 + \frac{b_0 + B}{2C} - \frac{\tan \alpha}{2Q_0} \left(\frac{V_{DC}}{V_{RF}} - 1 \right) \quad (6)$$

where ω_0 is the intrinsic frequency of a magnetron's cavity. Q_{ext} is the external quality factor, Q_0 is the intrinsic quality

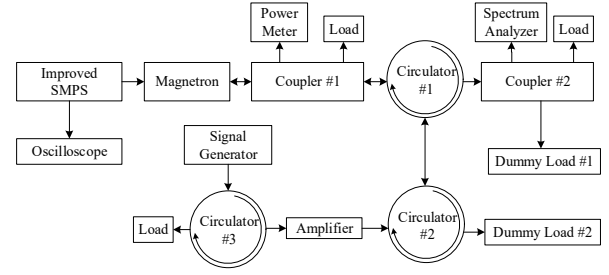


Fig. 3. Diagram of the experiment system.

factor. It is worth noting that when $d\theta/dt=0$, (5) will become the famous Adler's equation [15]:

$$|\Delta\omega| < \frac{\rho\omega_0}{Q_{ext}} \quad (7)$$

Similarly, by combining (2)-(4) and taking the real part of the equation, we will have the following:

$$V_{RF} = \frac{V_{dc}}{2RC\gamma \left(1 + \frac{\omega_0\rho \cos \theta}{Q_{ext}\gamma} \right)}, \gamma = \omega_0 \left(\frac{1}{Q_0} + \frac{1}{2Q_{ext}} \right) \quad (8)$$

where γ is defined as the growth factor [16]. (5), and shows an ILMGT's output phase and magnitude are still influenced by the power supply's DC voltage. The voltage ripple will deteriorate an ILMGT's output stability. It is important to suppress an ILMGT's anode voltage ripple to obtain a stable and purity output.

III. VOLTAGE RIPPLE SUPPRESSION METHOD

A. Voltage Ripple Suppression Module

Magnetron's anode voltage and current always have a close relationship. The current value will change with its voltage, and vice versa. Therefore, to reduce a magnetron's anode voltage ripple, one effective method is to control its current ripple. MOSFETs are devices that will control current based on their field effect. The maximum drain-source current is related to its gate-source current. In this case, if we design a module based on the MOSFETs output characteristic, nearly constant anode current control will be realized, and the magnetron's voltage ripple will be suppressed. Fig. 2(a) gives out the diagram of the active voltage suppression module we designed. This circuit is a closed-loop feedback circuit. A voltage regulator TL431 is used to provide a reference voltage, and the potentiometer R_t will adjust the input voltage of the operational amplifier's non-inverting input. The sample resistor R_f is used to sample the current and provide a feedback voltage to the inverting input of the operational amplifier. Then, the operational amplifier will provide the gate-source voltage of the MOSFET to control the circuit current.

In this section, the voltage ripple suppression method is carried out based on a commercial SMPS (WELAMP 2000F, Magmeet) and a 1kW, 2.45GHz magnetron (Panasonic 2M-210). The magnetron's maximum anode current generally does not exceed 420mA, and the typical value of the anode current is about 350mA. Thus, we set the maximum constant current value as 600 mA. The TL431's output voltage is set at 2.5V, and we chose the OP-07 operational amplifier, with $R_3=R_4=R_6=1k$, $R_f=2.2\Omega$, $R_2=R_f=1k\Omega$, and $R_5=220k$, to achieve effective feedback control of the gate voltage. The MOSFET is IRFP250.

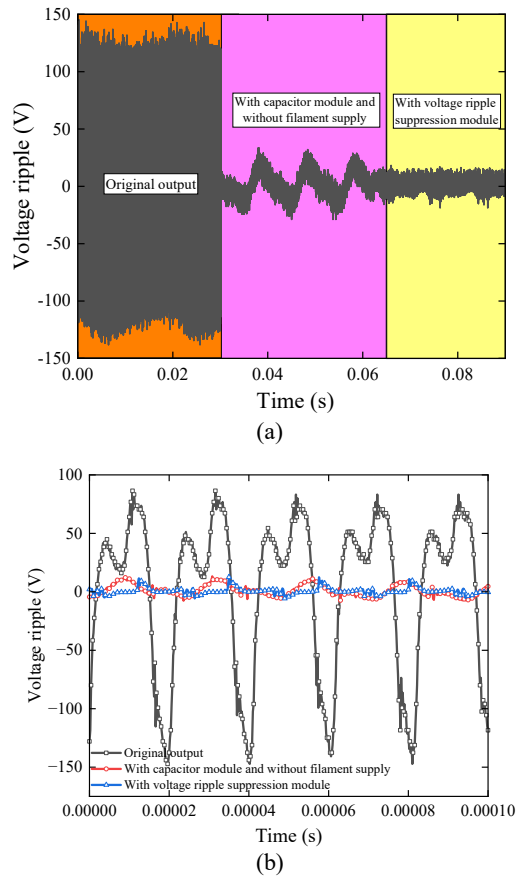


Fig. 4. Anode voltage ripple of the magnetron. (a) Total ripples. (b) High frequency ripples.

However, the SMPS we chose has a high-voltage ripple; the peak-to-peak value of the ripple is over 280 V. The voltage ripple suppresses module cannot completely eliminate the ripple independently because the MOSFET will break down and will affect the magnetron's operation. Therefore, we will combine this method with other methods.

B. Filament Control and Filter Module

The filament current supply of a magnetron plays an important role in the magnetron's output characteristic. It refers to the current used to heat the magnetron's cathode and increase electron emission. The filament current increases a magnetron's anode voltage ripple and deteriorates an ILMGT's output stability. For a 1-kW S-band cook-type magnetron, after it is operating stable, its filament current is verified that it can be reduced or turned off because its secondary electron emission is enough to hold its operating state. The SMPS we used has an AC filament, and it won't be cut off automatically. Thus, we add a relay module on the filament circuit. The relay module has a function that will turn off after a period which is a maximum of 60 seconds.

Filter module has demonstrated its improved effect on anode voltage ripple and magnetron's output [10]. The voltage ripple of an SMPS always contains two components: 1) dozens of kHz switch-frequency noise, and 2) 50 Hz and 100 Hz (in China) power frequency noise. To suppress the power frequency noise, it is necessary to apply large-volume capacitors and inductors, which are bulky and expensive. But for switch-frequency noise, only a small-volume and compact high-frequency capacitor is required. Therefore, we add a high-frequency capacitor module to the output of the SMPS;

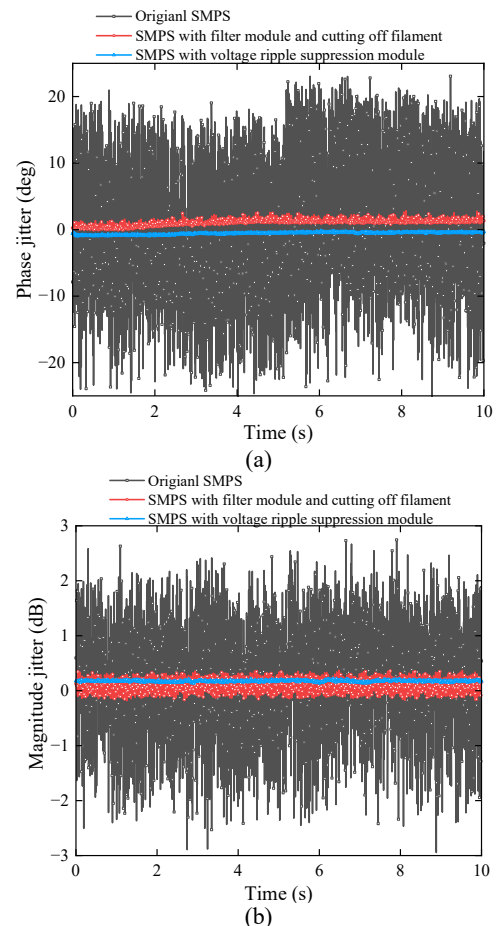


Fig. 5. Output characteristics of the injection-locked magnetron under different conditions. (a) Output phase jitter. (b) Output magnitude jitter.

its capacitance is about 0.25 μF . Fig. 2(b) shows a diagram of the SMPS improved by our active voltage suppression module, filament control module, and filter module. Fig. 2(c) shows the photograph of the improved SMPS; the proposed method just slightly increases the total size. The volume of the SMPS is increased from 2964 cm^3 to 3941 cm^3 .

IV. EXPERIMENT AND RESULTS

A. Experiment Setup

An experimental system has been established to verify our improvement in the SMPS and magnetrons' output. Fig. 3 shows the block diagram of the ILMGT experimental system. In this system, the magnetron is the Parasonic 2M-210, 1kW, 2.45GHz, which is consistent with our active voltage ripple suppression module design choices. This magnetron is powered by the improved SMPS (WELAMP 2000F, Magmeet). The diagram of the improved SMPS is represented by Fig. 2(b). The voltage ripple of the power supply is measured by a high-voltage probe (HVP-15HF, Pintek) and an oscilloscope (DPO-7254, Tektronix). A spectrum analyzer (FSP, R&S) is used to detect the magnetron's output spectrum, and the output power is measured by a power meter (AV2433). The injection signal is generated by a signal generator (HMC-T2220, Hittite) and a high-gain power amplifier (ZHL-30W-262, Mini-Circuits). The ILMGT's output phase is measured using a vector network analyzer (Agilent N5230A). The output microwave of the magnetron and the power coupled to the signal source due to reflection or imperfect isolation devices will be absorbed by a water-cooled dummy load.

B. Results and Discussion

Fig. 4 gives out the measured anode voltage ripple under different conditions. The peak-to-peak value of the SMPS is reduced significantly. The frequency of low- and high-frequency ripples are 100 Hz and 50 kHz, respectively. The total anode voltage ripple of the SMPS is 282V before improvement. After adding the filter module and cutting off its filament current, the voltage ripple still has a 62 V peak-to-peak value. The 50 kHz ripple is suppressed greatly by the high-frequency filter module, which is reduced from 223 V to 29 V. These results are consistent with our expectations. The reduction of the total ripple is mainly due to the filter module's suppression effect on high-frequency ripple. Then, when the compact voltage ripple suppression module is applied, the total ripple is decreased to 25 V, and the high-frequency ripple is reduced to 13 V. These results show the proposed module has an excellent effect on suppressing the low-frequency 100-Hz voltage ripple, and it also can reduce the 50kHz switch frequency noise. The proposed method is able to avoid the utilization of high-volume and bulky size low-frequency capacitors and inductors and is expected to be further improved to partially replace the high-frequency filter module.

Fig. 5(a) shows the output phase jitter of the ILMGT. Compared with Fig. 4(a), we will find the output phase jitter is reduced as the voltage ripple decreases, which is consistent with our theoretical analysis. The peak-to-peak value of the ILMGT's output phase jitter is reduced from 49° to 2.9° by filter module and filament current control and then suppressed to 0.7°. Similarly, as shown in Fig. 5(b), the output magnitude jitter is improved by the enhanced SMPS, too. The peak-to-peak value of its magnitude jitter is decreased from 5.6dB to 0.5dB and finally stabilized to 0.09 dB. These results indicate a high-stability IGMGT is realized based on an improved SMPS, but only with about a 32 % volume increase.

V. CONCLUSIONS

An injection-locked magnetron under the influence of anode voltage ripple is theoretically analyzed, and a commercial SMPS for magnetron is improved. A novel voltage ripple suppression module is designed, and combined with a high-frequency filter module and filament current control, the SMPS output anode voltage ripple is reduced significantly. The output stability of the ILMGT is also enhanced. After improvement, the anode voltage ripple is reduced from 282 V to 29 V, which results in a great improvement in the output phase and magnitude stability of the ILMGT. The output phase and magnitude jitter of the ILMGT are 0.7° and 0.09 dB. Our proposed novel voltage ripple suppression module provides a new approach to enhance the performance of an injection-locked magnetron. It is able to replace large-volume and high-cost low-frequency capacitors and inductors and partially instead of high-frequency filter components. This work indicates a compact and low-cost improvement method for SMPSs and is expected to establish high-stability ILMGT in various fields such as MWPT, phased arrays, etc.

ACKNOWLEDGMENT

The National Natural Science Foundation of China (NSFC) programs U22A2015 and 62071316 supported this work.

REFERENCES

- [1] Z. He and C. Liu, "A Compact High-Efficiency Broadband Rectifier With a Wide Dynamic Range of Input Power for Energy Harvesting," in *IEEE Microwave and Wireless Components Letters*, vol. 30, no. 4, pp. 433-436, April 2020.
- [2] B. Yang, X. Chen, J. Chu, T. Mitani and N. Shinohara, "A 5.8-GHz Phased Array System Using Power-Variable Phase-Controlled Magnetrons for Wireless Power Transfer," in *IEEE Transactions on Microwave Theory and Techniques*, vol. 68, no. 11, pp. 4951-4959, Nov. 2020, doi: 10.1109/TMTT.2020.3007187.
- [3] P. Anilkumar, A. Kumar, D. Pamu and T. Tiwari, "Design and Thermal Study of 5 MW S-Band Tunable Pulsed Magnetron for Linear Accelerator System," in *IEEE Transactions on Plasma Science*, vol. 51, no. 5, pp. 1223-1231, May 2023, doi: 10.1109/TPS.2023.3264813.
- [4] C. Liao, Y. He, Q. Chen and C. Liu, "Study on Microwave Drying Characteristic for PET Materials," 2022 IEEE MTT-S International Microwave Workshop Series on Advanced Materials and Processes for RF and THz Applications (IMWS-AMP), Guangzhou, China, 2022, pp. 1-3, doi: 10.1109/IMWS-AMP54652.2022.10107157.
- [5] S. Wang, Y. Shen, C. Liao, J. Jing and C. Liu, "A Novel Injection-Locked S-Band Oven Magnetron System Without Waveguide Isolators," in *IEEE Transactions on Electron Devices*, vol. 70, no. 4, pp. 1886-1893, April 2023.
- [6] I. Tahir, A. Dexter, and R. Carter, "Noise performance of frequency- and phase-locked CW magnetrons operated as current-controlled oscillators," in *IEEE Transactions on Electron Devices*, vol. 52, no. 9, pp. 2096-2103, Sept. 2005, doi: 10.1109/TED.2005.854276.
- [7] H. Huang, Y. Wei, X. Chen, K. Huang and C. Liu, "Simulation and Experiments of an S-Band 20-kW Power-Adjustable Phase-Locked Magnetron," in *IEEE Transactions on Plasma Science*, vol. 45, no. 5, pp. 791-797, May 2017, doi: 10.1109/TPS.2017.2689502.
- [8] T. Mitani, N. Shinohara, H. Matsumoto, and K. Hashimoto, "Improvement of Spurious Noises Generated from Magnetrons Driven by DC Power Supply after Turning off Filament Current", *IEICE Trans. Electron*, Vol. E86-C, No.8, pp.1556-1563, 2003
- [9] Z. Liu, X. Chen, M. Yang, K. Huang and C. Liu, "Experimental Studies on a 1-kW High-Gain S-Band Magnetron Amplifier With Output Phase Control Based on Load-Pull Characterization," in *IEEE Transactions on Plasma Science*, vol. 46, no. 4, pp. 909-916, April 2018, doi: 10.1109/TPS.2018.2814598.
- [10] X. Chen, Z. Yu, H. Lin, X. Zhao and C. Liu, "Improvements in a 20-kW Phase-Locked Magnetron by Anode Voltage Ripple Suppression," in *IEEE Transactions on Plasma Science*, vol. 48, no. 6, pp. 1879-1885, June 2020, doi: 10.1109/TPS.2019.2956868.
- [11] T. -S. Lee, S. -J. Huang, Y. -R. Lin, T. -C. Hung and C. -C. Chen, "Combination of Filament-Heating and Cavity-Driven Circuit With Gain-Frequency Regulation Control for Magnetrons," in *IEEE Transactions on Power Electronics*, vol. 36, no. 2, pp. 1921-1930, Feb. 2021.
- [12] S. -T. Han, D. Kim, J. Kim and J. -R. Yang, "Noise Suppression and Precise Phase Control of a Commercial S-Band Magnetron," in *IEEE Access*, vol. 8, pp. 145881-145886, 2020, doi: 10.1109/ACCESS.2020.3013651.
- [13] X. Chen, B. Yang, N. Shinohara and C. Liu, "Low-Noise Dual-Way Magnetron Power-Combining System Using an Asymmetric H-Plane Tee and Closed-Loop Phase Compensation," in *IEEE Transactions on Microwave Theory and Techniques*, vol. 69, no. 4, pp. 2267-2278, April 2021, doi: 10.1109/TMTT.2021.3056550.
- [14] J. C. Slater, "The phasing of magnetrons," *Res. Lab. Electron., MIT, Cambridge, MA, USA, Tech. Rep. TK7855.M41 R43 no.35*, April 1947.
- [15] Adler R. "A study of locking phenomena in oscillators," *Proceedings of the IRE*, vol. 34, no. 6, pp: 351-357, June 1946, doi: 10.1109/JRPROC.1946.229930.
- [16] S. C. Chen, "Growth and frequency pushing effects in relativistic magnetron phase-locking," in *IEEE Transactions on Plasma Science*, vol. 18, no. 3, pp. 570-576, June 1990, doi: 10.1109/27.55928.I. S. Jacobs and C. P. Bean, "Fine particles, thin films and exchange